Proceedings of the 37th IEEE
Conference on Decision & Control
Tampa, Florida USA • December 1998

Stability and sensitivity analysis of periodic orbits in Tapping Mode Atomic Force microscopy.

Murti V. Salapaka[1] , D. J. Chen
Electrical Engineering Department at Iowa State University
Ames Iowa 50011
J. P. Cleveland
Digital Instruments
Santa Barbara California 93117

Abstract

In this paper, the most widely used mode of atomic force microscopy imaging where the cantilever is oscillated at its resonant frequency is studied. It is shown that the amplitude and the sine of the phase of the orbit vary linearly with respect to the cantilever-sample distance. Experiments conducted on a silicon cantilever agree with the theory developed.

1 Introduction

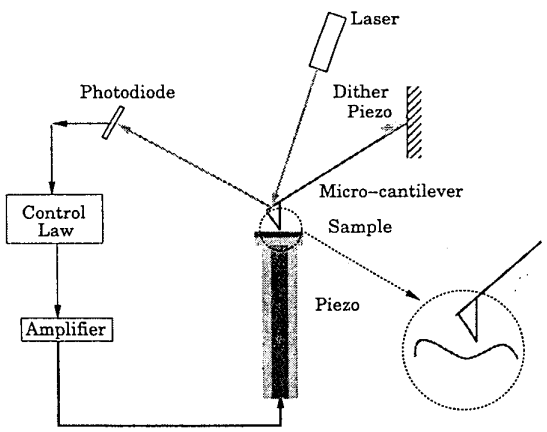

Figure 1: A schematic of an atomic force microscope. The sample to be imaged sits on a piezo tube which moves the sample in all three directions. As the sample is moved beneath the micro-cantilever, its deflections are registered by the resulting deflection of the laser incident on a photodiode.

The basic operating principle of an AFM is illustrated in Figure 1. A typical AFM consists of a micro-cantilever, a sample positioning system, a detection system and a control system. Sample positioning is provided by a piezoelectric actuator which can position the sample in two lateral directions and one vertical direction. As the sample is brought near the cantilever tip, the influence of the sample on the cantilever becomes significant enough to be registered by the detection system. A popular detection technique is based on the optical lever method where the laser incident on the top surface of the cantilever is deflected into a split photodiode sensor. Central to the operation described above is the cantilever which largely determines the achiveable sensitivity and resolution of the AFM. A typical cantilever is approximately hundred microns long, twenty microns wide and on the order of a micron thick. The cantilever tip can have dimensions approaching that of an atom.

Tapping Mode imaging is a relatively new method of imaging that overcomes many of the drawbacks of previous modes. In this mode the cantilever is oscillated near its resonant frequency using a piezoelectric crystal (the dither piezo in Figure 1). The profile of the sample has an influence on the characteristics of oscillations, which are monitored to identify and measure surface features. Here the cantilever tip is in contact with the sample for a very short time due to which the effect of the cantilever impact is minimal. Thus this mode has found widespread applications for imaging soft samples in both ambient conditions and under liquids. In *tapping mode* the cantilever tip moves through the whole range of the cantilever-sample potential which makes a linear model of this interaction inadequate [1]. Furthermore, it has been shown [2, 5] that chaotic behavior is possible due to the nonlinearity present. Experimental evidence for such behavior is also present [3].

In this paper a nonlinear dynamic model for the cantilever-sample interaction is first developed. With this model it is shown that the system exhibits periodic motion with period equal to that of the forcing. The Poincare map technique is used to establish asymptotic orbital stability of the periodic motion. Furthermore, the sensitivity of the Poincare map's fixed point with respect to the cantilever-sample distance is ob-

[1] This research was supported by NSF grant ECS-9733802

0-7803-4394-8/98 $10.00 © 1998 IEEE

tained. The fixed point consists of the amplitude and the "phase" of the periodic orbit, which can be measured from the cantilever vibration. The sensitivity study of the fixed point has shown that the amplitude and the sine of the phase of the orbit vary linearly with respect to the cantilever-sample distance. Experiments conducted on a silicon cantilever have shown that the cantilever motion is indeed periodic with period equal to that of the forcing. Furthermore, the variation of the amplitude and sine of the phase were recorded as the sample was moved towards the cantilever. The experimental data confirms the theoretically predicted linear behavior of these quantities with respect to the cantilever-sample distance.

2 Analysis of Tapping Mode imaging

A cantilever-sample interaction potential is derived in [2]. The cantilever-sample forces are characterized by long range attractive forces and short range repulsive forces. In ambient conditions capillary forces typically dominate the attractive portion of the potential [7]. A schematic of a typical potential between the cantilever and the sample is shown in Figure 2 which depicts the qualitative characteristics of the cantilever-sample interaction. The cantilever sample model is given by Figure 3, which shows a spring-mass-damper system as a model of the cantilever. The cantilever sample interaction is modeled as a nonlinear spring which is effective only after the separation between the cantilever and the sample is smaller than ℓ. The energy losses when the cantilever is under the influence of the sample are taken into account by a damping term $c(y, \dot{y})$. Thus the cantilever sample model is described by the following differential equation (where $x = (x_1,\ x_2)$),

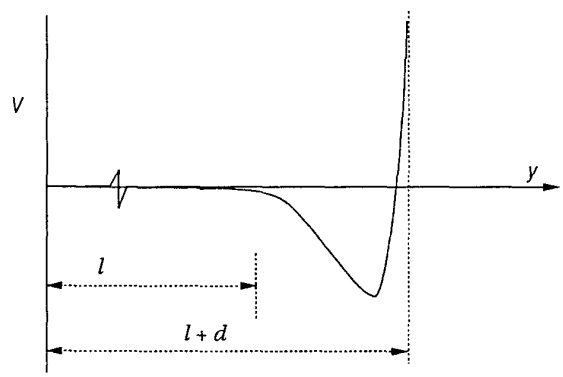

Figure 2: Sketch of a typical cantilever-sample potential. The sample has a long range attractive force which can be neglected after a separation ℓ. For short separations the forces are strongly repulsive. The force on the cantilever due to the sample is given by $-\frac{\partial V}{\partial y}$.

$$\dot{x} = \begin{pmatrix} x_2 \\ -2\xi\omega_0 x_2 - c(x_1, x_2) - k_0 x_1 - h(x_1) + g(t) \end{pmatrix}. \tag{1}$$

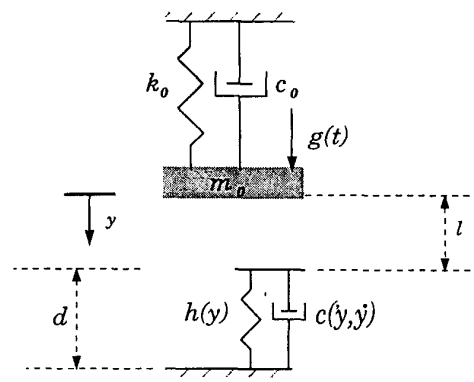

Figure 3: Model of the tapping mode cantilever and its interaction with the sample. The (k_0, m_0, c_0) system models the cantilever, attractive forces and the repulsive forces exerted by the sample are given by the nonlinear spring $h(y)$ and the nonlinear damper $c(y, \dot{y})$.

During Tapping Mode imaging a sinusoidal voltage is applied to the dither piezo (see Figure 1). Such a sinusoidal excitation can be modeled as an equivalent sinusoidal forcing on the mass in the spring-mass-damper model of the cantilever shown in Figure 3. The cantilever is first sinusoidally vibrated without the presence of the sample, till the cantilever has settled into periodic oscillations with frequency equal to that of the forcing. Once the steady state is reached the sample is moved towards the cantilever and the cantilever starts "tapping" the sample. This produces a change in the nature of the oscillations which relates to the properties like surface topography and hardness of the sample. Thus by monitoring the changes, material properties can be imaged; the remarkable feature being that data at the atomic scales are obtained.

When the cantilever is not in contact with the sample (that is the cantilever is in the region $\{y : y \leq \ell\}$) the potential force $h(y)$ and the sample damping $c(y, \dot{y})$ can be neglected. With these simplifications the dynamic equation for the cantilever "in air" is given by

$$\begin{pmatrix} \dot{x}_1 \\ \dot{x}_2 \end{pmatrix} = \begin{pmatrix} x_1 \\ -2\xi\omega_0 x_2 - k_0 x_1 \end{pmatrix} + \begin{pmatrix} 0 \\ 1 \end{pmatrix} g(t). \tag{2}$$

The following result establishes the existence of a periodic orbit.

Theorem 1 *The dynamics given by (1) with $g(t) = \gamma \cos \omega t$, has a periodic solution with a period $T = \frac{2\pi}{\omega}$, if the operating conditions are such that if anytime the*

cantilever enters the region $\{x_1 : x_1 \geq \ell\}$ then it leaves the same region with a velocity whose magnitude is smaller than the magnitude of the velocity with which it enters the region. Furthermore it is assumed that the sum of the spring force and the cantilever-sample interaction force on the cantilever is always repulsive (directed away from the sample).

The conditions for the existence of a periodic solution with the same period as that of the forcing function are mild. The only assumption made is that the velocity with which the cantilever tip enters the region where the sample's influence is not insignificant, is greater than the velocity with which it leaves the region. In the limit when the cantilever spends no time in the sample this assumption follows from the principle of conservation of energy. As will be discusssed later, the cantilever stays in the region $\{y : y \geq \ell\}$ for a small duration. Thus this assumption is not restrictive. This assumption can be further relaxed; the exiting velocity can be larger than the entering velocity but only within some given range.

We will use the Poincare map method to further analyse the dynamics. The Poincare section is characterized by the position of the highest point the cantilever will reach in each cycle and the time at which it reaches the highest point. The fixed point of the Poincare map is directly related to the magnitude of the periodic oscillation. This allows us to study the sensitivities of the periodic orbit with respect to various parameters important for imaging. Once the stability of the fixed point is established we will study the sensitivity of the fixed point with respect to the cantilever-sample distance, which is given by ℓ.

For the Tapping Mode dynamics, $g(t) := \gamma \cos \omega t$. The two dimensional Poincare section we will consider is given by

$$\Sigma = \{(x_1, x_2, t) : x_1 \leq 0, x_2 = 0, t \in R^+\}. \quad (3)$$

Let the periodic orbit Γ^* corresponding to the periodic solution whose existence was proven in Theorem 1 intersect the Poincare section Σ at $p^* = (t^*, x^*)$ in $R \times R^2$. The normal to the Poincare section Σ is characterized by the vector $(0\ 1\ 0)'$ (because for any vector $(x_1, x_2, t)'$ in Σ, $(0\ 1\ 0)(x_1, x_2, t)' = 0$). The Poincare section will be transversal to the periodic orbit Γ^* at p^* if $(0\ 1\ 0)'\tilde{f}(p^*)$ is not equal to zero. This is true if $\omega_0^2 x_1^* \neq \gamma \cos \omega t$. We will establish later that for normal operating conditions of the Tapping Mode atomic force microscope, $\omega_0^2 |x_1^*| >> \gamma$. Thus the periodic orbit is transversal to Σ.

Let U a subset of Σ be a sufficiently small neighbourhood of p^* such that Γ intersects U only once. We now construct the Poincare map which maps U into Σ. The second coordinate is always zero for any element in Σ. For notational brevity we will drop this coordinate for the rest of the discussion. For a point (y_0, t_0) in U ((y_0, t_0) is identified with $(y_0, 0, t_0)$) the map $P(y_0, t_0)$ is defined by the following operations.

Let $x(t_0) = (y_0, 0)$ and let the components of the solution $\varphi(t, t_0, x(t_0))$ of (2) with initial condition specified at time t_0 as $x(t_0)$ be denoted by $(x_1(t)\ x_2(t))'$ (where x_1 and x_2 represent the position and the velocity respectively). Let $t_\downarrow > t_0$ be the smallest time such that $x_1(t_\downarrow) = \ell$. Denote the velocity $x_2(t_\downarrow)$, by $\dot{y}_\downarrow$. Let P^1 represent the map given by,

$$P^1 : \begin{pmatrix} y_0 \\ t_0 \end{pmatrix} \rightarrow \begin{pmatrix} \dot{y}_\downarrow \\ t_\downarrow \end{pmatrix}. \quad (4)$$

Let $x(t_\downarrow) = (\ell, \dot{y}_\downarrow)$ and let the solution $\varphi(t, t_\downarrow, x(t_\downarrow))$ of (1) with initial condition specified at time $t_\downarrow$ as $x(t_\downarrow)$ be denoted by $(x_1\ x_2)$. Let $t_\uparrow > t_\downarrow$ be the smallest time such that $x_1(t_\uparrow) = \ell$. Denote the velocity $x_2(t_\uparrow)$ by $\dot{y}_\uparrow$. Let P^2 represent the map given by

$$P^2 : \begin{pmatrix} \dot{y}_\downarrow \\ t_\downarrow \end{pmatrix} \rightarrow \begin{pmatrix} \dot{y}_\uparrow \\ t_\uparrow \end{pmatrix}. \quad (5)$$

Finally with initial conditions $x(t_\uparrow) = (\ell, \dot{y}_\uparrow)$ for (2) let P_3 represent the map

$$P^3 : \begin{pmatrix} \dot{y}_\uparrow \\ t_\uparrow \end{pmatrix} \rightarrow \begin{pmatrix} y_f \\ t_f \end{pmatrix}, \quad (6)$$

where $t_f > t_\uparrow$ is the smallest time when the velocity is zero and y_f is the position at this time. The Poincare map $P : U \rightarrow \Sigma$ is defined by

$$P := P^3 \circ P^2 \circ P^1, \quad (7)$$

and thus $P((y_0, t_0)) = (y_f, t_f)$.

Implicit in the construction of the Poincare map is the assumption that for all elements of U the cantilever goes through the stages described by P^1, P^2 and P^3. We assume that the velocity of the mass m_0 (shown in Figure 3) on the periodic orbit Γ^* towards the sample at the position $\ell + d$ is nonzero. From continuity of solutions with respect to initial conditions we know that there exists a neighbourhood of p^* in Σ such that any trajectory with initial conditions in the neighbourhood will have a nonzero velocity at the position $\ell + d$. This ensures that U can be chosen small enough so that for all elements of U the cantilever goes through the stages described by P^1, P^2 and P^3.

Theorem 2 *The periodic orbit of (1) with a period $T = \frac{2\pi}{\omega_0}$ for $g(t) = \gamma \cos \omega_0 t$ is stable if the following assumptions on the periodic orbit hold;*

1. *the cantilever leaves the region* $\{x_1 : x_1 \geq \ell\}$ *with a velocity whose magnitude is lesser than the magnitude with which it enters the same region,*
2. *the periodic orbit exits the region* $\{x_1 : x_1 \geq \ell\}$ *instantaneousl,*
3. *the time when the velocity is positive is equal to the time when the velocity is negative,*
4. *the damping* $\xi << 1$.

Assumption 1 in the theorem statement is mild; it can be further relaxed based on the damping factor ξ. Assumption 2 has been discussed at the begining of this part of the section. It is expected that assumption 3, that the time of flight from x_0 to ℓ given by $t_\downarrow - t_0$ is equal to the time of flight from the position ℓ back to the Poincare section which is given by $t_f - t_\uparrow$, if the periodic orbit meets the sample when its velocity is near zero. This characteristic of the steady state orbit is supported by experimental evidence. Assumption 4 is true for most atomic force opertaing conditions. It needs to be stressed that these assumptions are made only on the steady state periodic orbit and they can be violated during transients. Also, the stability is based on the eigenvalues of the Jacobian of the Poincare map P. As the eigenvalues are continuous with respect to the entries of the Jacobian, the stability result can be expected to hold even if the conditions are near but not exactly the same as the ones specified by the assumptions.

2.1 Amplitude and phase of the periodic orbit

In the tapping mode imaging the surface profile of the sample is imaged based on the amplitude of the cantilever oscillation. Imaging techniques also utilize the phase between the periodic orbit and the forcing with an implicit assumption that the orbit can be approximated by a sinusoid. In this part of the paper we obtain analytical relationships between the maximum magnitude of the cantilever oscillation and the sample cantilever distance ℓ. We also obtain the phase of the periodic orbit with respect to the forcing, at a displacement farthest from the sample.

Note that for the periodic orbit, $y(t_\downarrow) = \ell$. Differentiating this equation with respect to ℓ and obtaining an expression for the derivative of $\dot{y}(t_\downarrow)$ with respect to ℓ, we have,

$$\begin{pmatrix} 1 & -\ddot{y}_\downarrow \\ 0 & -\dot{y}_\downarrow \end{pmatrix} \begin{pmatrix} \frac{D\dot{y}_\downarrow}{D\ell} \\ \frac{Dt_\downarrow}{D\ell} \end{pmatrix} = \begin{pmatrix} \frac{\partial \dot{y}_\downarrow}{\partial y_0} & \frac{\partial \dot{y}_\downarrow}{\partial t_0} \\ \frac{\partial y_\downarrow}{\partial y_0} & \frac{\partial y_\downarrow}{\partial t_0} \end{pmatrix} \begin{pmatrix} \frac{Dy_0}{D\ell} \\ \frac{Dt_0}{D\ell} \end{pmatrix} + \begin{pmatrix} 0 \\ -1 \end{pmatrix}.$$

If we assume that the time spent "in the sample" (that is in the region $\{y : y \geq \ell\}$) in each cycle of the periodic orbit is small and that the velocity $\dot{y}_\uparrow = -\lambda \dot{y}_\downarrow$, we have

$$\begin{pmatrix} \frac{D\dot{y}_\uparrow}{D\ell} \\ \frac{Dt_\uparrow}{D\ell} \end{pmatrix} = \begin{pmatrix} -\lambda & 0 \\ 0 & 1 \end{pmatrix} \begin{pmatrix} \frac{D\dot{y}_\downarrow}{D\ell} \\ \frac{Dt_\downarrow}{D\ell} \end{pmatrix}. \tag{8}$$

Finally note that $\dot{y}_f = 0$. Differentiating this equation with respect to ℓ and obtaining an expression for the derivative of y_f with respect to ℓ, we have,

$$\begin{pmatrix} 1 & 0 \\ 0 & \ddot{y}_f \end{pmatrix} \begin{pmatrix} \frac{Dy_f}{D\ell} \\ \frac{Dt_f}{D\ell} \end{pmatrix} = \begin{pmatrix} \frac{\partial y_f}{\partial \dot{y}_\downarrow} & \frac{\partial y_f}{\partial t_\downarrow} \\ \frac{\partial \dot{y}_f}{\partial \dot{y}_\downarrow} & \frac{\partial \dot{y}_f}{\partial t_\downarrow} \end{pmatrix} \begin{pmatrix} \frac{D\dot{y}_\uparrow}{D\ell} \\ \frac{Dt_\uparrow}{D\ell} \end{pmatrix} + \begin{pmatrix} \frac{\partial y_f}{\partial \ell} \\ 0 \end{pmatrix}$$

Note that on the periodic orbit $y_f = y_0$ and $t_f = t_0$. Thus, we can use the above three Equations to obtain $\frac{Dy_0}{D\ell}$ and $\frac{Dt_0}{D\ell}$. Thus under the assumptions of Theorem 2 we have,

$$\frac{Dy_0(\ell)}{D\ell} \approx -k_\ell, \tag{9}$$

and

$$\frac{D\phi}{D\ell} \approx -k_\phi \frac{\omega_0^2 \ell + \gamma \cos\phi}{-\omega_0^2 y_0(\ell) + \gamma \cos\phi} \frac{1}{\cos\phi}. \tag{10}$$

where $\phi = \omega_0 t_0$, $k_\ell = \frac{(\lambda+1)e^{-\xi\pi}}{\lambda + e^{2\xi\pi}}$, and $k_\phi = \frac{\delta\omega}{\gamma} \frac{(\lambda+1)e^{2\pi\xi}(1+e^{\xi\pi})}{(\lambda+e^{2\xi\pi})^2}$. If we restrict the operation of the AFM to a region where $\ell >> 2\xi\ell_0$ where $\ell_0 = \frac{\gamma}{\delta}\omega$ is the amplitude of the sinusoidally forced cantilever without the sample present, then $\omega_0^2 \ell >> 2\xi\omega_0^2 \ell_0 cos\phi = \gamma \cos\phi$. Also, note that as ξ is very small k_ℓ can be approximated by one. Thus $|y_0(\ell)|$ can be approximated by ℓ from which it follows that

$$\frac{D \sin\phi}{D\ell} \approx -k_\phi. \tag{11}$$

Thus these relations predict a linear relationship of the maximum deflection of the cantilever and the phase (as defined before) with respect to the cantilever sample separation.

We had mentioned before that a sufficient condition for the transversality of the Poincare section to the periodic solution, is that $\omega_0^2|y_0| \neq \gamma \cos\omega t$ where (t_0, y_0) is the point where the periodic solution meets the Poincare section. Note that if ℓ_0 denotes the amplitude of vibration of the cantilever under the forcing $\gamma \cos\omega_0 t$ without the sample's influence then $\frac{\omega_0^2 \ell_0}{\gamma|\cos\omega_0 t|} = \frac{1}{2\xi} >> 1$ (as $\ell_0 = \frac{\gamma}{\delta\omega_0}$). Thus $\omega_0^2 \ell_0 >> \gamma|\cos\omega_0 t|$ Note that from (9) it follows that $|y_0(\ell)|$ can be approximated by ℓ. Thus, $\omega_0^2|y_0(\ell)| \approx \omega_0^2 \ell$ from which it follows that $\omega_0^2|y_0(\ell)| >> \gamma \cos\omega_0 t$ for values of ℓ sufficiently near ℓ_0.

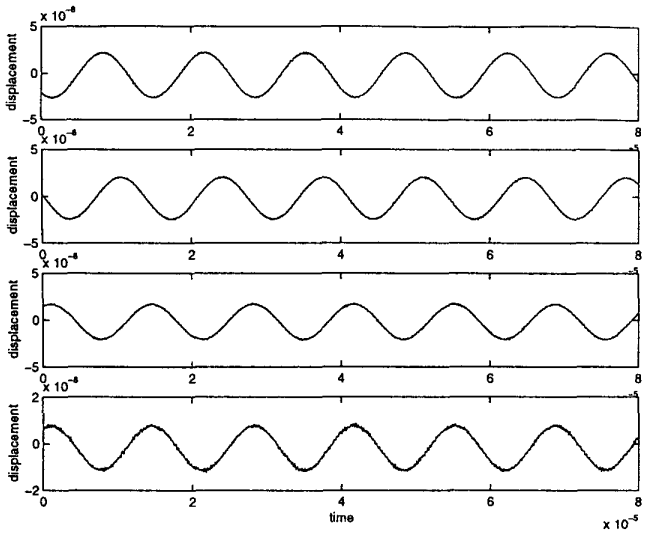

Figure 4: Cantilever deflection vs. distance

3 Experimental results

An atomic force microscope (MultiMode, Digital Instruments, Santa Barbara, CA) was operated in the Tapping Mode. A silicon cantilever of length 225 microns was used. The model parameters were evaluated by analysing the cantilever response to thermal noise in similar ways to the those suggested in [4, 6]. The quality factor Q of the cantilever was evaluated to be 130, (Q is given by $\sqrt{k_0 m_0}/c_0$). Thus we have $\xi = \frac{1}{2Q} = \frac{1}{260} = 0.0038$. The first modal frequency of the cantilever was at $\omega_0 = 2\pi \times 73881$ rad/sec. For the one mode model, the stiffness k_0 was found to be 4 N/m.

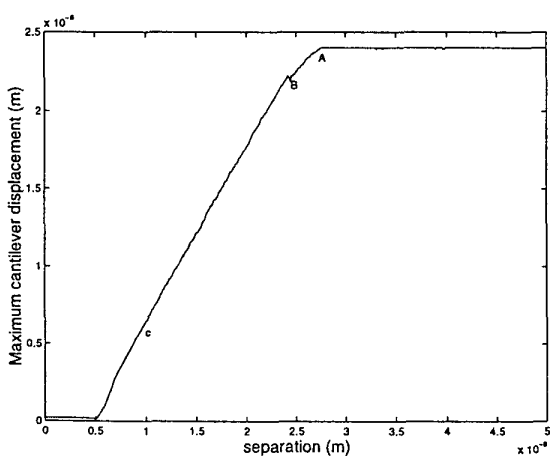

Figure 5: The plot of the maximum cantilever tip deflection with respect to piezo extension.

A sinusoidal voltage with its frequency equal to the resonant frequency ω_0 of the cantilever was applied to the

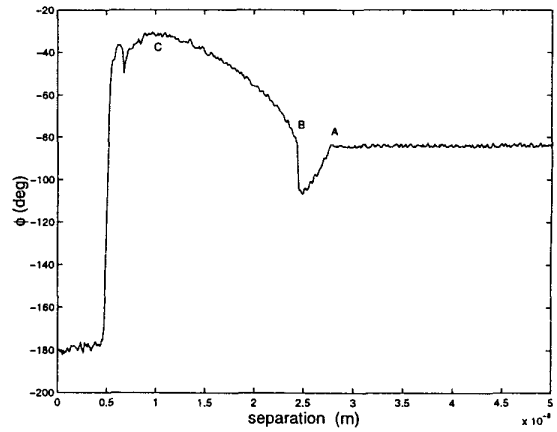

Figure 6: Phase Vs. distance.

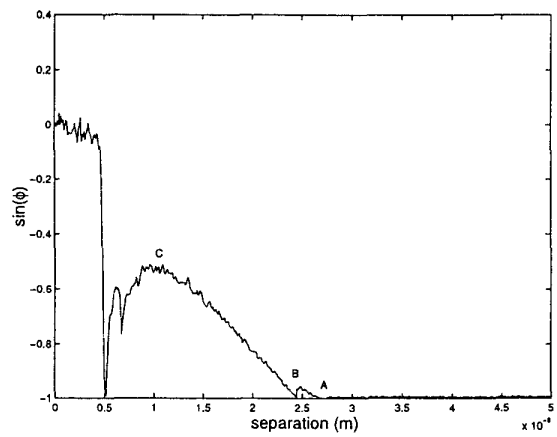

Figure 7: $\sin(\phi)$ Vs. piezo extension.

dither piezo (see Figure 1). The sample (slicon wafer) initially was sufficiently far from the cantilever so that it did not affect the cantilever motion. Once the cantilever reached its steady state (after $\approx 1ms$), the sample was slowly moved towards the vibrating cantilever by extending the piezo (see Figure 1).

The motion of the cantilever tip at various values of the piezo extension, was recorded using HP 89410 Vector Signal Analyzer. Time series plots of the steady state behavior of the cantilever tip at different piezo positions are shown in Figure 4. As established by Theorem 1 and Theorem 2 we see that the cantilever tip is on a periodic orbit. The time period of the orbits determined from the plots is equal to $\frac{2\pi}{\omega_0}$. A spectrum analysis of the data shows that the orbits are nearly sinusoidal when the cantilever sample separation is large. When the cantilever separation is smaller, the cantilever motion deviates slightly more from a sinusoidal behavior.

The piezo extension with respect to the voltage applied to the piezo scanner is linear in the relevant range (less

than one percent deviation). It needs to be stressed that the only quantifiable control on the sample and the cantilever tip separation is through the piezo extension. There is no separate measure of the cantilever and the sample separation. However, it can be assumed that there is a constant offset between piezo extension and the cantilever sample separation. With this understanding the horizontal axis is labeled "separation" in Figures 5, 6 and 7.

The amplitude of the cantilever at various values of the separation are given in Figure 5. Since the oscillations are nearly sinusoidal the amplitude can be approximated by the maximum displacement. The phase between the cantilever tip motion (approximated by a sinusoid) and the forcing was also obtained experimentally (see Figure 6). It is evident from Figure 5 that the maximum deflection of the cantilever varies linearly with respect to the separation, in the region between points B and C (see Figure 5). Also, in Figure 7, $\sin(\phi)$ is plotted against the separation. As can be seen, the experimental data shows that the plot is linear between the points B and C.

When the piezo extension is between the points marked A and B the cantilever tip barely (if at all) penetrates the repulsive region of the potential. The attractive region of the potential (see Figure 2) has considerable influence on the cantilever motion. For values of the piezo extension less than that given by A the cantilever is not influenced by the sample and for values of the piezo extension more than that given by C the tip probably never leaves the moisture layer present on the surface. For purposes of the analysis presented here the appropriate region of the piezo extension is between the points B and C. As is evident the plots of $\sin(\phi)$ and the maximum displacement are linear in this region which corroborate the analytically obtained expressions in relations (9) and (11). Experiments conducted on a wide variety of samples show similar characteristics as illustrated in the experiment described in this paper.

This study has anlaytically shown, with support from experimental data that $\sin(\phi)$ and the maximum magnitude of the cantilever displacements can be effectively utilized to map the topography of the sample. This study also suggests that material properties like coefficient of restitution can be obtained by utilizing the plot of $\sin(\phi)$ with respect to cantilever sample separation though better models for cantilever sample interaction need to be employed.

4 Conclusions

In this paper a nonlinear dynamic model was introduced to describe the Tapping Mode atomic force microscope. Based on the model the existence of periodic orbits under mild conditions was proven. Using the Poincare method the asymptotic orbital stability of the periodic solution was established. The sensitivity of the amplitude and the sine of the phase of the cantilever vibration revealed a linear relationship with respect to a parameter ℓ which characterizes the cantilever-sample distance.

Experiments using a silicon cantilever were performed. The parameters for the cantilever model developed were found using the response of the cantilever to thermal noise. Under a sinusoidal forcing the cantilever response was periodic with the period equal to that of the forcing; corroborating the theoretical results. Furthermore, as predicted by the analysis, the amplitude and the sine of the phase of the cantilever vibration were linear with respect to cantilever sample separation.

Ongoing research has indicated that other tools (e.g. harmonic balance and averaging) from dynamics and control literature can be very useful in understanding the Tapping Mode dynamics and for developing newer modes of imaging.

References

[1] B. Anczykowski, D. Kruger, K. L. Babcock, and H. Fuchs. Basic properties of dynamic force spectroscopy with scanning force microscope in experiment and simulation. *Ultramicroscopy*, 66/3-4, 1997.

[2] M. Ashhab, M.V. Salapaka, M. Dahleh, and I. Mezic. Dynamical analysis and control of microcantilevers. *accepted to Automatica.*

[3] N. A. Burnham, A. J. Kulik, G. Gremaud, and G. A. D. Briggs. Nanosubharmonics: the dynamics of small nonlinear contacts. *Physics Review Letters*, 74:5092–5059, 1995.

[4] M. V. Salapaka, H. S. Bergh, J. Lai, A. Majumdar, and E. McFarland. Multimode noise analysis of cantilevers for scanning probe microscopy. *Journal of Applied Physics*, 81(6):2480–2487, 1997.

[5] S. W. Shaw and P. J. Holmes. A periodically forced piecewise linear oscillator. *Journal of Sound and Vibration*, 90(1):129–155, 1983.

[6] D. A. Walters, J. P. Cleveland, N. H. Thomson, P .K. Hansma, et al. Short cantilevers for atomic force microscopy. *Review of Scientific Instruments*, vol.67, no.10:3583–90, 1996.

[7] A. L. Weisenhorn, P. K. Hansma, T. R. Albrecht, and C. F Quate. Forces in atomic force microscopy in air and water. *Applied Physics Letters*, 54, no.26:2651–3, 1989.